Influence of Ash Agglomerating Fluidized Bed Reactor Scale-Up on Coal Gasification Characteristics

Yuncai Song, Jie Feng, Yalong Jia, and Wenying Li
Key Laboratory of Coal Science and Technology (Taiyuan University of Technology), Ministry of Education and Shanxi Province, Taiyuan 030024, P.R. China

Yitian Fang
Institute of Coal Chemistry, Chinese Academy of Science, Taiyuan 030001, P.R. China

DOI 10.1002/aic.14379
Published online February 7, 2014 in Wiley Online Library (wileyonlinelibrary.com)

To study the influence of fluidized-bed reactor scale-up on coal gasification characteristics, a model of the ash agglomerating fluidized-bed reactor has been developed using an equivalent reactor network method. With the reactor network model, the scale-up effects of a gasifier were studied in terms of the characteristics of the chemical reactions in the jet zone, the annulus dense-phase zone and the freeboard zone. Results showed that the changes occurred in the inequality proportion of the volume of the jet zone during the reactor scale-up. Taking into consideration the utilization of a portion of the backflow gas, the expansion of the jet zone volume and the coal particle residence time, the temperature of the jet zone was increased from 1592 to 1662 K. Also, both the annulus dense-phase zone temperature and the freeboard zone temperature decreased, causing subsequent decrease in the carbon conversion efficiency. © 2014 American Institute of Chemical Engineers *AIChE J*, 60: 1821–1829, 2014
Keywords: reactor scale-up, equivalent reactor network model, pilot-scale gasifier, coal gasification characteristics

Introduction

Ash agglomerating fluidized-bed gasifier (AFB),[1–4] such as U-GAS® and KRW, is considered as one of the most effective reactors to handle coal with higher ash content and ash fusion temperature. AFB has the advantages of moderate operating temperature, lower oxygen consumption, and flexibility of feedstock. Nevertheless, AFB has to be operated at near ash slagging temperature conditions to prevent ash agglomerating at the bottom of the gasifier.[5] To optimize reactor running and scale-up, many studies[6–8] on the aspects of hydrodynamics, reaction kinetics, and gasification performance provide a great deal of information about particle hydrodynamic behavior and heat/mass transfer under different operating conditions. However, during the reactor scale-up process from lab/pilot-scale to commercialized scale process, the thermochemical properties which affect the product gas composition will change, presenting some serious difficulties, such as heat transfer between ash and feedstock at the dense phase area.

It is well known that it is a daunting task for a process engineer to scale up a reactor.[9,10] Matsen[11] has pointed out that "scale-up is still not an exact science but is rather that mix of physics, mathematics, witchcraft, history, and common sense that we call engineering." Traditionally, a reactor scale-up process based on empirical judgment is used to scale-up the reactor from a bench-scale process to a pilot-scale and finally to industrial-scale. If the scale-up reactor process involves chemical reactions or a multiphase of gas, liquid, and solid, it is more difficult to explain the scale-up effect of the scale-up reactor process through empirical judgment. If deterioration of the reaction results is discovered in the empirical judgment-based scale-up process, then it can be said that a scale-up effect exist in the process. However, the method of the empirical judgment-based scale-up process cannot explain which factors caused the scale-up effects, or how they could be diminished. Additionally, numerous factors ranging from raw materials to product handling must be taken into account at every level of the empirical-based scale-up, which requires much more time and resources.[12,13] Compared with the above approach, the principle of similarity scale-up could simplify the reactor scale-up process by determining the main dimensionless groups characterizing the process phenomenon.[14] Some researchers[15,16] have investigated a full set of hydrodynamics scaling parameters for fluidized-bed reactor scale-up. However, the chemical reaction process is affected not only by hydrodynamics but also by heat transfer, mass transfer and chemical reactions.[13,17] In practice, in a reactor scale-up, it is necessary to maintain as much as possible the consistency of diffusion, hydrodynamics, heat transfer, and chemical reactions. However, it is virtually impossible to keep all the dimensionless groups characterized by a similarity of diffusion, hydrodynamics, heat transfer and chemical reactions as the number of dimensionless groups is enormous and there is always the presence of conflict between the different dimensionless groups.[14] For example, the ratio of the reactor length to the linear velocity of the mixture in reactor ($L_{reactor}/U_{mixture}$) should be kept

Correspondence concerning this article should be addressed to J. Feng at fengjie@tyut.edu.cn and W. Li at ying@tyut.edu.cn.

constant to insure similarity in the chemical reactions, also assuring consistency in hydrodynamics and diffusion. Therefore, balancing these factors during the scale-up process in gasifier design is of great importance.

Computational fluid dynamics (CFD) has become a powerful tool to study the hydrodynamics of a reactor scale-up. According to other studies, [13,16,18–21] with the CFD simulation method, the influence of the special reactor structure on the hydrodynamic characteristics can be studied through cold-state simulation. Also, the internal mass and temperature distribution of a kilogram-scale reactor can be studied by simplifying the chemical reactions within the reaction mechanism. Fluid dynamics will affect mass transfer, heat transfer, momentum transfer, and the chemical reactions. In addition, continuously occurring chemical reactions will lead to changes in fluid flow. In this circumstance, it is difficult to predict the problems that may be encountered during the reactor's scale-up process. The calculation results cannot be obtained due to a rapid growth of the number of Navier-Stokes differential equations. In another words, the CFD simulation can obtain results for the kilogram scale but not for the kiloton scale because of the corresponding mesh count for the commercial-scale reactor will be appreciably larger than that for the smaller-scale reactors, especially for coal gasification processes.[19,22–24] During the coal gasification process, not only the hydrodynamics but also the coal particle size, density, and shape, change with the coal gasification reactions, making the gasification process much more complex than the CFD calculations. In such cases, in order to avoid solving the above mentioned difficulties, reasonable simplifications must be done which can focus on the critical problems in the chemical process of reactor scale-up. For the scale-up process of the reactor, it is necessary to determine how the mass/heat/momentum transfers affect the chemical reactions in consideration of the major fluid flow zones of the reactors. Although the gasification process is very complex, the main gasification reactions which occur in the fixed-bed gasifier, fluidized-bed gasifier and entrained-bed gasifier have been studied.[25–27] In this case, it would be possible to devise a new method of studying the AFB gasifier scale-up by combining different types of idealized reactors [e.g., plug flow reactor (PFR), continuous stirred tank reactor (CSTR)] to equate real reactors. This was done by first analyzing the complicated chemical reaction processes of the mass/heat/momentum transfer in the partially oxygenized environment of the jet zone in both the jetting fluidized-bed gasifier and in the reduction environment of the freeboard zone. Then, on the basis of previous experiments, calculations of the fluid dynamics, and the gasification reaction process of different zones within the reactor and the volume changes of the fluid dynamic zones proceeding and following the scale-up of the reactor were carried out. With this method, it is hoped that an understanding of the causes of the changes in the thermal chemical environment in the AFB gasifier scale-up process can be obtained.

In this study, an equivalent reactor network model of the ash agglomerating fluidized-bed reactor was set up based on results from experiments on gasifier with a 300-mm inner diameter using CHEMKIN 4.0 software has the capacity to combine calculations for hydrodynamics, heat/mass transfer as well as the reaction kinetics. The influences of operation parameters and reactor shape parameters on each regions' heat/mass transfer and chemical reactions were studied with the developed model, particularly analyzing the change in mass between the jet zone and the annulus dense-phase zone during the reactor scale-up. This article specifically examines the effect the scale-up of ash agglomerating fluidized-bed reactors on coal gasification characteristics, taking into consideration the coal particles' hydrodynamics and chemical reactions in order to gain further insight into the causes of gas composition fluctuation in the reactor scale-up process.

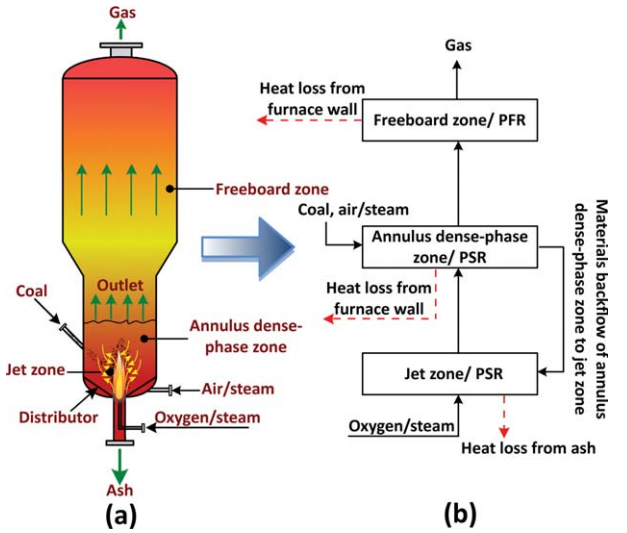

Figure 1. Schematic of AFB and its equivalent reactor network.

Equivalent Reactor Model Setup

Model description

The equivalent reactor network model is established on the basis of the AFB reactor (ID = 300 mm) developed by the Institute of Coal Chemistry, the Chinese Academy of Sciences. The AFB gasifier structure has been previously described in detail.[28]

The CHEMKIN model was set up based on the previous research. First, the kinetic parameters of coal were obtained. Second, the reaction zones were divided on the basis of previous experiments and the fluid dynamics and gasification reaction process of different zones within the reactor were calculated. The specific process includes: zone division, calculation of zone volume, similarity analysis of the fluid flow types in all zones and the idealized reactor, transfer process analysis of energy and mass between zones, determination of transfer equation of mass/heat, balanced calculation of whole reactor's mass/heat. A detailed description follows.

Determination of reaction zone division

Based on hydrodynamics calculation of the previous AFB,[8,20,24,29] the gasifier was divided into three parts, the jet zone, the annulus dense-phase zone and the freeboard zone,[30] and the combined equivalent reactor is illustrated in Figure 1a. In the jet zone, where the gas and solid are well mixed, a perfectly stirred reactor (PSR) is used to simulate this zone. Around the jet zone, there occurs a strong materials exchange between the jet zone and the annulus dense-phase zone. Thus, the annulus dense-phase is assumed as the PSR in the model. In the freeboard zone, it is assumed that both the gas flow and the particle flow are in a plug flow

state so it is taken as the PFR[26,31] in the model of the freeboard zone. Additionally, the backflow of materials between the annulus dense-phase zone and the jet zone is taken into account in the model. Combined with the hydrodynamics of AFB reactor, the equivalent reactor network model of the AFB reactor is built, as shown in Figure 1b, including the heat/mass transfer as well as the chemical reaction in the different regions.

Model calculation principle in CHEMKIN

Taking into consideration the hydrodynamic characteristics, the chemical reactions and also the conservation of mass, energy, and momentum between individual reactors, a combination of ideal reactors was used to represent a nonideal reactor, aiming at approaching the process of the nonideal reactors. The equations of PSR and PFR in CHEMKIN 4.0 including mass continuity, energy conservation, and compositions conservation are calculated as follows.[32]

The mass continuity equation of PSR

$$\frac{d(\rho V)}{dt}=\sum_{k=1}^{N_{\text{inlet}}}\dot{m}_k^*-\dot{m} \tag{1}$$

The compositions conservation equation of PSR

$$\frac{dY_k}{dt}=\frac{\dot{m}}{\rho V}(Y_k^*-Y_k)+\frac{\dot{\omega}_k W_k}{\rho} \tag{2}$$

The energy conservation equation of PSR

$$c_p\frac{dT}{dt}=\frac{\dot{m}}{\rho V}\sum_{k=1}^{K}Y_k^*(h_k^*-h_k)-\sum_{k=1}^{K}\frac{h_k\dot{\omega}_k W_k}{\rho}+\frac{\dot{Q}}{\rho V} \tag{3}$$

The mass continuity equation of PFR

$$\rho u\frac{dA}{dx}+\rho A\frac{du}{dx}+uA\frac{d\rho}{dx}=\sum_{m=1}^{M}a_{i,m}\sum_{k=1}^{K_g}\dot{s}_{k,m}W_k \tag{4}$$

The energy conservation equation of PFR

$$\rho uA\left(\sum_{k=1}^{K_g}h_k\frac{dY_k}{dx}+c_p\frac{dT}{dx}+u\frac{du}{dx}\right)+\left(\sum_{k=1}^{K_g}h_kY_k+\frac{1}{2}u^2\right)\sum_{m=1}^{M}a_{i,m}\sum_{k=1}^{K_g}\dot{s}_{k,m}W_k=a_eQ_e-\sum_{m=1}^{M}a_{i,m}\sum_{k=K_b^f}^{K_b}\dot{s}_{k,m}W_kh_k \tag{5}$$

The momentum conservation equation of PFR

$$A\frac{dP}{dx}+\rho uA\frac{du}{dx}+\frac{dF}{dx}+u\sum_{m=1}^{M}a_{i,m}\sum_{k=1}^{K_g}\dot{s}_{k,m}W_k=0 \tag{6}$$

The gas-phase conservation equation of PFR

$$\rho uA\frac{dY_k}{dx}+Y_k\sum_{m=1}^{M}a_{i,m}\sum_{k=1}^{K_g}\dot{s}_{k,m}W_k=W_k\left(\sum_{m=1}^{M}\dot{s}_{k,m}a_{i,m}+\dot{\omega}_kA\right) \tag{7}$$

Determination of model parameters

The Parameters of the Jetting Zone. As described in previous research,[6] the ratio of the inlet nozzle diameter to the gasifier diameter (d_{or}/D_t) is a significant parameter for the gas-solid mixing hydrodynamic characteristics and there is no obvious changes in the jet zone when d_{or}/D_t is in the range of 0.08–0.12. In this work, d_{or}/D_t was taken to be 0.10. However, the volume of reactor does not have a linear relationship with the inlet nozzle diameter. According to the empirical formula, the inner diameter of reactor, the feedstock flow rate of the reactor and the reactor temperature all limit the design of the inlet nozzle diameter. The formula is as follows

$$d_{or}=\lambda\times f(D_t,\ Q_{\text{oxygen}},\ Q_{\text{steam}},\ T_{jet}) \tag{8}$$

where λ is the nozzle design coefficient, d_{or} (m) and D_t (m) are the inlet nozzle diameter and gasifier inner diameter, respectively, Q_{oxygen} ($\text{Nm}^3\ \text{h}^{-1}$) is the total oxygen feed flow rate, Q_{steam} (kg h^{-1}) is the total steam feed flow rate and T_{jet} (K) is the jet zone temperature.

The jet zone diameter is given as follows[33,34]

$$\frac{d_{\text{j}}}{d_{\text{or}}}=1.56\left(\frac{f_iF_{\text{rj}}}{\sqrt{k}\tan\varphi_r}\right)^{0.3}\left(\frac{d_{\text{or}}}{D_t}\right)^{0.2} \tag{9}$$

When

$$f_i\approx 0.02, F_{rj}=\frac{\rho_{\text{g}}u_{or}^2}{(1-\varepsilon_{mf})\rho_{\text{s}}d_{\text{p}}g}, k=\frac{1-\sin\phi_r}{1+\sin\phi_r}$$

where d_{j} (m) is the jet zone diameter, and u_{or} (m s^{-1}) is the jet velocity at the nozzle. d_{p} (m) and ρ_{s} (kg m^{-3}) are the particle diameter and density, respectively, and ρ_{g} (kg m^{-3}) is the gas density. ε_{mf} is the voidage of the bed at minimum fluidization and φ_{r} (rad) is the cone angle. F_{rj}, k, and f_{i} are the constants defined in Eq. 9.

The jet zone depth is calculated as follow[35]

$$\frac{h_{\text{j}}}{d_{\text{or}}}=15.0\left(\frac{\rho_{\text{g}}}{\rho_s-\rho_{\text{g}}}\frac{{u_{\text{or}}}^2}{gd_{\text{or}}}\right)^{0.187} \tag{10}$$

where h_{j} (m) is the jet zone depth.

The volume of the jet zone is used

$$V_{\text{j}}=\frac{\pi}{4}h_{\text{j}}d_{\text{j}}^2 \tag{11}$$

where V_{j} (m^3) is the jet zone volume.

The Parameters of the Annulus Dense-Phase Zone. The volume of the annulus dense-phase is calculated as follows

$$V_{\text{d}}=\frac{\pi}{4}h_{\text{j}}(D_t^2-d_{\text{j}}^2) \tag{12}$$

where V_{d} (m^3) is the annulus dense-phase zone volume.

It is essential to understand the material exchanges between the jet zone and the annulus zone in the scale-up reactor process. Luo et al.[8] and Bi and Kojima[34] studied on the jetting fluidized bed gasifier which had a great similarity with the AFB gasifier, they have taken into the consideration of the annulus temperature contributing to ash agglomeration and the mass exchange equations between the jet zone and the annulus zone. Thus, in present study, the materials backflow rate was taken into account.

The backflow rate of gas from the annulus dense-phase zone to the jet zone depends on the radial gas velocity and the superficial area of the jet zone.[35,36] The gas exchange rate (U_{ex}) between the jet zone and the annulus dense-phase zone is used as an index to evaluate the amount of the backflow of gas from the annulus dense-phase zone to the jet zone. Deduced from Eqs. 3–7 as published by Bi and Kojima,[34] the U_{ex} is described as follows

$$U_{ex} = K \cdot \frac{1}{2} \cdot \frac{S_a u_{mf}}{d_j h_j} \left(\sin \frac{\pi h}{2h_j}\right)^{-0.5} \cdot \cos \frac{\pi h}{2h_j} \quad (13)$$

where K is the coefficient of gas exchange between the annulus dense-phase zone and the jet zone, and K is calculated as follows[8]

$$K = u_d^{0.48} u_{or}^{0.36} \quad (14)$$

where S_a (m^2) is the cross-sectional area of the annulus dense-phase zone. u_{mf} (m s^{-1}) is the minimum fluidizing gas velocity and u_d (m s^{-1}) is the gas velocity from the distributor shape.

The solid mass backflow rate from the annulus dense-phase zone to the jet zone is calculated as follows[34]

$$\frac{W_s}{W_{s,h_j}} = \frac{h}{h_j}\left(2 - \frac{h}{h_j}\right) \quad (15)$$

$$W_{s,h_j} = 12.5 W_{g0} \quad (16)$$

where W_s (kg s^{-1}) is the laterally entrained particle flow rate and its amount changes with height. $W_{s,hj}$ (kg s^{-1}) is the solids mass flow rate at the top of the jet zone and W_{g0} (kg s^{-1}) is the gas mass flow rate from the nozzle. h (m) is the axial distance from nozzle.

The Equivalent Process of Coal Sample. It is well recognized that coal has a complicated structure and any simulation software cannot input the components without explicit structure. So, in order to satisfy the calculation process, the coal sample input must be simplified. Before gasification, the coal is pyrolyzed to coal char, ash, and volatiles including H_2O, CO, CH_4, and H_2. Therefore, based on the elements and energy balance through these processes, with the addition of energy, the coal sample can be substituted by C(s), ash, H_2O, CO, CH_4, and H_2.[36] The total substitution of coal should satisfy the elements and energy balance in the process of the coal pyrolysis unit. The presence of coal particles of different sizes presents certain difficulties in investigation. For example, fine particles may fly away with the ash, or coarse particles may be involved in the ash's aggregation. Therefore, the capacity to investigate the particle-size distribution in the scale-up reactor process is still limited. In the calculations, an average diameter of 0.5 mm was used for the coal particles, which references indicate is the most probable particle size of raw coal used in the AFB gasifier.[28]

The Computation Process of Energy Conservation. The computation process of energy conservation of each zone in the gasifier has been detailed in previous work.[30] The heat loss caused by the sensible heat of ash (Q_{ash}) is formulated as follows

$$Q_{ash} = m * \Delta T \overline{C}_p \quad (17)$$

$$\overline{C}_p = \sum_{i=1}^{7} C_{pi} x_i \quad (18)$$

where m^* (kg) represents the total amount of ash and ΔT (K) is the temperature change of ash. C_{pi} (J kg^{-1} K^{-1}) and $\bar{C}_p$ (J kg^{-1} K^{-1}) are the heat capacity of each ash component and the mean heat capacity of ash components. x_i is the mass fraction of each component in ash.

The specific ash components, such as SiO_2, Al_2O_3, Fe_2O_3, CaO, SO_3, MgO, and TiO_2, are taken into account in the calculations reported elsewhere.[30] The coal ash mass fraction in this article contains 43.09% SiO_2, 29.83% Al_2O_3, 15.99% Fe_2O_3, 5.28%CaO, 0.80% MgO, 1.24% TiO_2, 2.75% SO_3, 0.78% K_2O, 0.08% Na_2O, and 0.09% P_2O_5.

Statement of reactor scale-up process

The independent variables of coal gasification are the coal, steam, and oxygen mass flow rates. When three variables are fixed, the reactor temperature and the gas composition should be obtained. Whereas the frequency factor (k_s), the activation energy (E), the residence time (t), the reactor temperature (T), and each component in the reactor concentration (c_i) determine the gasification rate. Other factors, such as the feedstock properties and the structure of the reactor, act upon the coal gasification indirectly. Thus, to keep the chemical reaction as similar as possible to the reactor scale-up, it must be assured these parameters k_s, E, t, T, and c_i are maintained as constant as possible. However, it is infeasible to maintain all the parameters constant in the reactor scale-up. k_s and E both depend on the coal char properties and could be regarded as constant in the reactor scale-up. To keep parameter t unchanged, the ratio of the reactor volume to the total feedstock flow rate should be invariant. However, the parameters T and c_i are related to both the extent of the chemical reactions and also the heat/mass transfer and cannot be adjusted in the experiment. Therefore, to maintain the T and c_i constant as far as possible in the reactor scale-up process, both the initial concentration and the preheat temperature of reactants should be kept invariable.

The key assumptions in the scale-up reactor are as follows

1. The AFB gasifier is composed of three zones: the jet zone, the annulus dense-phase zone, and the freeboard zone. In the process of scale-up, the hydrodynamic types of individual zones remain invariable but the volume of each changes as does the mass/heat transfer between different zones.
2. The constants in the coal gasification kinetic network model do not change in the scale-up process.

In this gasifier scale-up project, the coal obtained from Shanxi Province of China was selected as the feedstock. The proximate and ultimate analyses of coal are shown in Table 1. The AFB reactor with inner diameter of 300 mm is marked as S and reactor with a 600 mm inner diameter as L. The detailed structure sizes of reactor S and L are shown in Table 2. An expansion of the interior in the gasifier means the increase in capacity, correspondingly, the amount of feedstock and the volume of the gasifier should be expanded under the constraints of heat and mass balance. That is, the amount of coal input should be sufficient to maintain a stable temperature in the gasifier whose length meets the residence time requirements necessary to achieve full combustion. On this basis, the reactor length was set up as twice the original size, and the inlet nozzle diameter was enlarged from ϕ30 to ϕ60 mm. It was found that the volume of L could enlarge up to eight times the volume of S, so the reactor volume scale-up coefficient (β) was taken to be 8. As above-mentioned, to keep the initial parameter t constant, all of the feedstock mass flow rates in L were enlarged to eight times in S (the total feedstock scale-up coefficient β_1 is 8) so that the impact of gasification reaction condition would be maintained as constant as possible.

Table 1. The Proximate and Ultimate Analysis of Coal

	Proximate Analysis (wt %)				Ultimate Analysis (wt %)				
Sample	$M_{t,ar}$	A_{ar}	FC_{daf}	V_{daf}	C_{ar}	H_{ar}	O_{ar}	N_{ar}	$S_{t,ar}$
coal	6.8	13.76	91.12	8.88	72.39	2.63	3.08	1.00	0.34

Notes: M_t - the total moisture; A - the ash, FC - the fixed carbon; V - the volatiles; C - the carbon element; H - the hydrogen element; O - the oxygen element; N - the nitrogen element; S_t - the total sulfur element; ar - as received basis; daf - dry ash free basis.

Changes in the physical size and handling capacity of the reactor would result in changes in the volume of the jet zone, the annulus dense-phase zone and the freeboard zone in the scale-up reactor. The volume of each zone is the key input parameter when doing calculations with the CHEMKIN software. Volume changes in different zones will lead to the changes in the materials' residence time, in mass, heat, and momentum transfers, and thus in the temperature and products distribution of the scale-up reactor.

Reactions

It is well known that during the coal gasification process, pyrolysis, volatile release, heterogeneous char reactions, and homogeneous reactions of the gas phase all occur instantaneously.

The establishment of the coal gasification reaction kinetics is a basic problem in the coal chemical industry. Essentially, the kinetics parameters are the basis of the design of coal gasification reactor, but the coal gasification process includes two reactive processes of coal pyrolysis and the following semichar gasification. The macro kinetic equations should combine these two reactions, and one equation should contain a form of expression for the process rate study. It was here assumed that the kinetic constants of char reactions satisfy the Arrhenius equation

$$K_f = k_s T^{\beta} \exp\left(\frac{-E}{RT}\right) \tag{19}$$

However, the parameters necessary for the reactor design are not obtainable through use of macro kinetics and must be obtained from intrinsic kinetics instead. Furthermore, coal is a nonhomogeneous material, whose kinetic characteristics in the reactive process can be represented by combining the characteristics of several hybrid materials and integrating their kinetic parameters. Some researchers[37,38] expressed this concept using a distribution activation energy model to describe its kinetic characteristics of coal gasification in different temperature ranges. In addition, the mass transfer in the reactor is also studied. As a result, the kinetic parameters of different studies[39–48] and different reactors seem very inconsistent with one another and relevant adjustment should be made per specific conditions of utilization. Fortunately, in fluidized-bed reactors or entrained gasifiers of a sufficiently high temperature, the influence of thermodynamics factors on the reaction process is much greater than kinetic factors.

Table 3 summarizes reaction equations and corresponding reaction rate constants—some kinetic parameters from the laboratory scale ID 60 mm fluidized-bed reactor[49] and others from the literatures[23,39–41]—used in the equivalent reactor network model. These parameter values are chosen for the following reasons. The first reason is to ensure conservation of mass and energy in the model calculation process; the second is that the calculation results are close to the data from the 300-mm gasifier operated in self-heating mode. It is assumed that there would be that no significant changes in the kinetic parameters if the diameter of the reactor were extended to 600 mm: in the process of reactor scale-up, k_s and E are kept invariant.

Results and Discussion

Model validation

The calculated product gas composition, carbon conversion efficiency results, and corresponding experimental results are shown in Table 4. A simulation results that are in agreement with experimental data can be obtained by the reaction network model, also the calculation time can be ignored. This indicates that appropriate simplification does not ruin the gasifier model but gives a faster and acceptable result. The gas component contents are within a 3% margin of error and the carbon conversion efficiency is nearly the same value for both the calculation and experiment. Therefore, the adopted kinetic constants could represent the experimental reaction conditions. These kinetic constants were assumed to remain unchanged proceeding and following the scale-up process. Then, the effect of changes in the reactor's structure, size, and feedstock amount on each of the zones' volumes, and influence of the resulting mass/heat/momentum transfer and chemical reactions on the reactor's temperature, and product compositions can be studied.

Changes in characteristics of the three zones in the reactor scale-up

Jet Zone in the Reactor Scale-Up. The jet zone, where the exothermic oxidation reactions occur, supplies the heat to the gasifier and gasification reactions. The higher proportion of feedstock in the jet zone taking part in the combustion reaction will cause a higher temperature in the jet zone.

Table 2. Operation Parameters and Reactor Size of S and L

Operation Conditions	S	L	Reactor Size (mm)	S	L
Operating pressure (MPa)	0.51	0.51	Diameter of gasifier	300	600
Coal feed flowrate (kg h^{-1})	81.75	654.00	Expanded diameter	500	1000
Air feed flowrate (Nm^3 h^{-1})	79.14	633.12	Height of gasifier	4740	9480
Steam feed flowrate of distributor (kg h^{-1})	104.03	832.24	Inlet nozzle diameter	30	60
Steam feed flowrate of loop pipe (kg h^{-1})	11.02	88.16			
Steam feed flowrate of nozzle (kg h^{-1})	5.90	47.20			
Oxygen feed flowrate of nozzle (Nm^3 h^{-1})	31.54	252.32			

Table 3. Reaction Equations and Corresponding Reaction Rate Constants

Reaction Equation	k_s (homogeneous unit)	E (kJ mol^{-1})	Literatures Cited
$C + O_2 \rightarrow CO_2$	1.10×10^{11}	92.78	49
$C + CO_2 \rightarrow 2CO$	8.10×10^{8}	121.42	49
$C + H_2O \rightarrow CO + H_2$	1.85×10^{2}	54.01	49
$C + 2H_2 \rightarrow CH_4$	1.25×10^{2}	96.41	49
$2CO + O_2 \rightarrow 2CO_2$	3.09×10^{8}	99.76	23
$2H_2 + O_2 \rightarrow 2H_2O$	8.83×10^{11}	99.76	23
$CO + H_2O \rightarrow CO_2 + H_2$	2.78×10^{6}	12.56	41
$CO_2 + H_2 \rightarrow CO + H_2O$	26.5	32.99	41
$CH_4 + H_2O \rightarrow CO + 3H_2$	1.65×10^{11}	329	40
$CH_4 + 2O_2 \rightarrow CO_2 + H_2O$	3.55×10^{17}	130.54	39

Hence, as the temperature approaches the point at which ash will melt, the ash will gradually clump together and begin to separate from the coal char due to difference in density. Therefore, controlling the jet zone temperature is a key factor in assuring the stable discharge of the ash.

Tables 5 and 6 show the critical parameters and component conversion efficiencies in the jet zones of S and L, respectively. In the process of reactor scale-up, the gas backflow rate from the annulus dense-phase zone to the jet zone varied from 48.28 to 271.71 kg h^{-1} after S enlarged to L, as shown in Table 5. Obviously, compared with the reactor volume scale-up coefficient β (=8), the gas backflow rate scale-up coefficient β_2 ($\beta_2 = 271.71/48.28$ kg h^{-1}) is not linearly scaled-up during the reactor scale-up process and is less than β. Thus, the lower amount of feedstock in the jet zone leads to a decline in the jet zone temperature after scale-up.

In the process of scale-up from S to L, the volume of the jet zone enlarged from 1378 to 28840 cm^3 (Table 5) and the jet zone volume scale-up coefficient (β_3) was calculated to be 21. As described previously, the total feedstock mass flow rate only to eight times of the original flow rate. All of these results cause the average reaction time in the jet zone to increase from 0.048 to 0.154 s after the reactor scale-up.

The longer residence time assists in the complete combustion of carbon, as shown in Table 6, the conversion efficiencies of carbon and oxygen increased from 66.42 and 1.47% to 84.40 and 1.91%, respectively. It promotes the jet zone temperature of L. This indicates that compared with the pilot-scale reactor, the bench-scale reactor is more difficult to readily operate.

Furthermore, Table 5 shows the variance in the mass of the components in the jet zone before and after reactor scale-up. The amount of coal particles recycled from the annulus dense-phase to the jet zone increases from 599 to 4795 kg h^{-1}, enhancing the heat transfer between the two zones. The temperature of the jet zone increases from 1592 to 1662 K after scale-up, which will increase the reaction rate by approximately 14 to 28 times according to the Van't Hoff rule. So, temperature change caused by increase in the jet zone volume plays an important role in the scale-up of the gasifier. To preserve similarity in the composition of the gas products, the stabilization of the jet zone volume must be considered. Increase in the temperature of the jet zone may cause ash melting and slagging problems in the AFB gasifier operation. So as to satisfy the constraints of the ash-melting temperature of coal (1724 K), the nozzle design coefficient λ value should be 4.87×10^{-9} and 3.12×10^{-7} for S and L, respectively. The inlet nozzle diameter is dependent on the feed rate of the reactor. The precondition for the inlet nozzle diameter adjustment is that no significant changes could occur to the hydrodynamic characteristics of the jet zone and that the inlet nozzle diameter should not increase beyond the range mentioned in the article. Otherwise the gas velocity into the jet zone might be such that the requisite gasifier temperature is not achieved and consequently gas compositions would also not be as required down the length of the reactor. The change in the inlet nozzle diameter has a direct influence on the jet zone diameter and depth, thus resulting in a volume change of the jet zone. The residence time in the jet zone is increased, generating an effect on the chemical reactions of the jet zone and the material and heat exchanges between the jet zone and the annulus dense-phase zone. The temperature of the jet zone increases from 1592 to 1662 K after scale-up, when these values are put into formula (8), the λ values are 3.37×10^{-7} and 5.10×10^{-9}, respectively. Therefore, in the process of reactor scale-up, to decrease the jet zone temperature, which would ensure the stabilization of the AFB gasifier operation, a method of increasing the steam to oxygen ratio in the inlet nozzle, for example, decreasing the amount of oxygen in the inlet nozzle, could be adopted. Also, to keep the λ value in the range of $4.87 \times 10^{-9} - 3.12 \times 10^{-7}$, the diameter of the inlet nozzle could be adjusted, which would also cause the jet zone temperature to decrease.

Table 4. Comparison of Calculated and Experimental Results

	Calculated Value	Experimental Value	Error
CO (mol %)	21.47	20.25	1.22
H_2 (mol %)	33.66	30.86	2.8
CO_2 (mol %)	20.87	22.87	2.00
CH_4 (mol %)	1.68	1.20	0.48
N_2 (mol %)	22.32	24.81	2.49
Carbon conversion efficiency (%)	89.97	90.12	0.15
Temperature (K)	1369	1293	74

The Annulus Dense-Phase Zone and the Freeboard Zone in the Reactor Scale-Up. The temperature profiles of S and L along the axial height are shown in Figure 2. The amount of oxygen consumed in the jet zone in S is lower than that in L which can be seen from the oxygen conversion efficiency in Table 6. Correspondingly, the ratio of the amount of oxygen residue to the amount of coal being input into the

Table 5. Variation of Mass in the Jet Zone Before and After Reactor Scale-Up

	Backflow Rate of Gas Phase (kg h^{-1})	Backflow Rate of Solid Phase (kg h^{-1})	Jet Zone Volume (cm^3)	Residence Time (s)	Mole Fraction of O_2 (%)	Jet Zone Temperature (K)
S	48.28	599	1378	0.048	12.52	1592
L	271.71	4795	28840	0.154	7.06	1662

Table 6. Comparison of Composition Inlet and Outlet Mass Flow Rate of Reactor S and L in the Jet Zone

	Inlet Mass Flow Rate (g s^{-1})		Outlet Mass Flow Rate (g s^{-1})		Conversion Efficiency (%)	
	S	L	S	L	S	L
CO	2.08	11.56	0.0069	0.039		
H_2	0.16	0.9	0	0		
CO_2	3.63	20.09	14.57	131.37		
H_2O	4.56	24.48	7.81	46.68		
CH_4	0.16	0.86	0.015	0.079		
N_2	3.67	20.23	3.67	20.23		
O_2	12.36	98.88	4.15	15.43	66.42	84.4
C(s)	166.42	1322.0	163.97	1296.81	1.47	1.91

annulus dense-phase is decreased after reactor scale-up. Thus, after scale-up, a decrease in the degree of combustion will lead to a decrease in the temperature of the annulus dense-phase and the freeboard phase.

In the process of the reactor scale-up, the annulus dense-phase volume is raised from 32,671 cm^3 in the S reactor to 277,343 cm^3 in the L reactor. The annulus dense-phase volume scale-up coefficient β_4 ($\beta_4 = 277{,}343\ cm^3/32{,}671\ cm^3$) is larger than the total feedstock scale-up coefficient β_1 (=8) so that the feedstock residence time of the annulus dense-phase would be increased. The carbon conversion efficiency of the annulus dense-phase rises from 63.48% in S to 64.14% in L in the reactor scale-up, as shown in Figure 3. However, as the temperature of the freeboard of S is lower that of L, as seen in Figure 2, the carbon conversion efficiency of the freeboard zone is decreased after reactor scale-up, which can be observed from Figure 3.

The calculated gas compositions of the two gasifiers are shown in Table 7. The temperature decline in the annulus dense-phase zone and the freeboard zone after scale-up are not beneficial to either the CH_4 reforming reaction ($CH_4 + H_2O = CO + 3H_2$), the Boudouard Reaction ($C + CO_2 = 2CO$), or the water-gas reaction ($C + H_2O = CO + H_2$), but the water-gas shift reaction ($CO + H_2O = CO_2 + H_2$) is enhanced. Thus, the comprehensive results show a slight increase in the CH_4 content, CO_2 content, H_2 content but a decrease in the CO content. The temperature and the feedstock residence time of both the annulus dense-phase zone

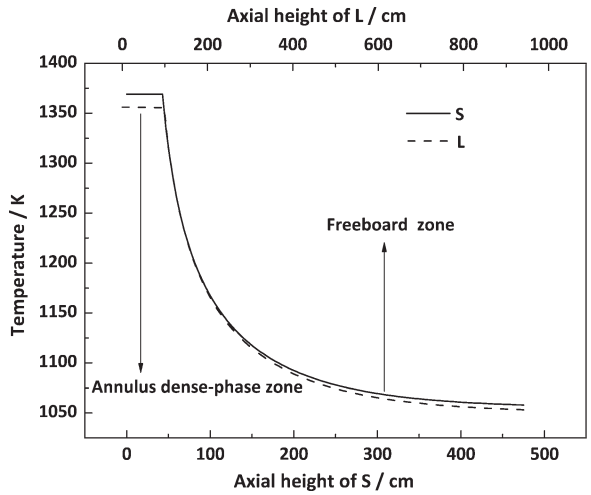

Figure 2. Temperature distribution along the axial height in reactor S and L.

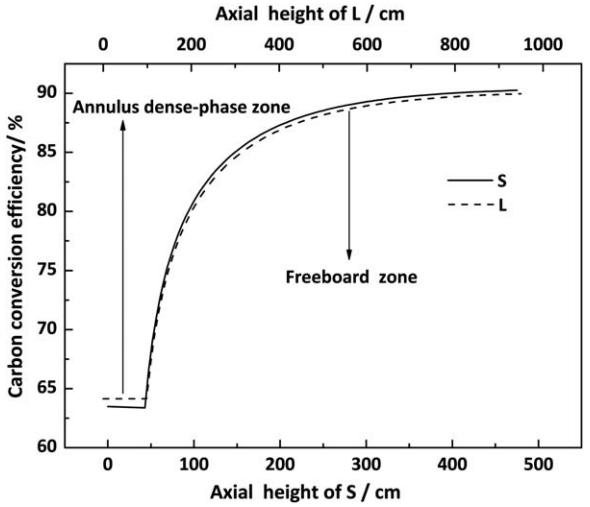

Figure 3. Axial carbon conversion efficiency of reactor S and L.

and the freeboard zone are key factors in affecting change in the gas composition and carbon conversion efficiency.

The hydrodynamics characteristics in the reactor scale-up process

As described in the introduction, much research[12,13,16,18,21,22,50–52] has been done to investigate the characteristics of hydrodynamics in the reactor scale-up process through either the hydrodynamics similarity approach or using the CFD simulation method. A set of hydrodynamics scale-up parameters in the bubbling bed was derived by Horio[52] based on the governing equation of bubbles and interstitial gas dynamics. Additionally, Glicksman[13,51] and He[50] provided a set of hydrodynamics scaling parameters for the spouting bed. Utilizing the scaling parameters of hydrodynamics for bubbling beds and spouting beds, Wang[22] modified the scaling parameters to better understand the scale-up of jetting fluidized beds on the basis of a hydrodynamic two-fluid model combined with the CFD simulation method. Thus, in this article, the hydrodynamic scaling parameters proposed by Wang were used to analyze the hydrodynamics characteristics of S and L. The physical parameters and dimensionless groups of S and L are shown in Table 8. It was found that there was good agreement in three of the dimensionless groups, $gd_p/(u_{mf})^2$, $\rho_g u_{mf} d_p/\mu_g$, and ρ_g/ρ_s, between the scale-up reactor and the original reactor. However, both the u_j/u_{mf} and the d_{or}/d_p dimensionless groups lacked agreement between S and L. These results confirm that it is impossible to keep all the dimensionless groups characterized by the similarity of hydrodynamics when maintaining consistency in the heat and chemical reactions. Combined with the results of the gasifier temperature, gasification composition, and carbon conversion as discussed in section on Changes in characteristics of the three zones in the reactor scale-up, for the scale-up of AFB, the

Table 7. Variation in Coal Gas Composition Before and After Reactor Scale-Up (mol %)

	CH_4	CO_2	CO	H_2
S	1.68	20.87	21.47	33.66
L	1.71	20.89	21.41	33.70

Table 8. The Physical Parameters and Dimensionless Groups of Reactor S and L

	$\frac{gd_p}{u_{mf}^2}$	$\frac{\rho_g d_p u_{mf}}{\mu_g}$	$\frac{\rho_g}{\rho_s}$	$\frac{u_j}{u_{mf}}$	$\frac{d_{or}}{d_p}$
S	10.15	0.23	0.0014	564.53	60
L	10.15	0.23	0.0014	1129.05	120

dimensionless groups u_j/u_{mf} and d_{or}/d_p of hydrodynamics are not significant in assuring stable operation of the AFB in the reactor scale-up process.

Conclusions

In the process of the AFB gasifier scale-up, the jet zone volume does not follow a linear increase. The extended residence time of the raw material in the jet zone enhances carbon combustion which results in a temperature increase in the jet zone. However, for the AFB, the operation temperature must be near the ash fusion temperature. If the gasifier temperature is higher than the ash fusion temperature, it may affect the ash-clinker discharge of the AFB gasifier reactor. At the same time, a rise in the jet zone temperature will cause an increase of CO_2 concentration with more CO_2 transferred to the annulus dense-phase zone and the upper-stage freeboard zone, leading to changes in the product composition. Thus, these results should be balanced in the reactor scale-up. Also, a decrease in the gas backflow rate from the annulus dense-phase to the jet zone and the increase in the jet zone volume result in an increase in the residence time of the feedstock in the jet zone and a decrease in the percent of feedstock combusted. The increased temperature of the jet zone in the larger scale reactor causes problems with slagging and operational difficulties in the AFB gasifier. Moreover, an increase in the consumption of oxygen in the jet zone in the larger scale reactor lead to a decrease in rate of the backflow of oxygen from the jet zone to the annulus dense-phase. The decreases in temperature in both the annulus dense-phase and in the freeboard zone in the larger scale reactor affect the carbon conversion efficiency and gas composition. The equivalent reactor network model developed in this research represents a tool for scale-up analysis that maintains similarity in heat/mass/momentum transfer and chemical reaction characteristics.

Acknowledgments

The authors thank the financial support provided by the NNSF of China (No. 21076136, 51276120), Shanxi Provincial NSF (2011011005-1), the Program for Changjiang Scholars (2009) and the Doctoral Supervisor (20101402110013, 20121402110016) in the Ministry of Education, P. R. China. The authors thank Sarah Enslow for English proofreading and editing.

Notation

Symbols

$L_{reactor}$ = the reactor length, m
$U_{mixture}$ = the linear velocity of the mixture in reactor, m s^{-1}
d_{or} = the inlet nozzle diameter, m
D_t = the gasifier inner diameter, m
Q_{oxygen} = the total oxygen feed flow rate, Nm^3 h^{-1}
Q_{oxygen} = the total steam feed flow rate, kg h^{-1}
T_{jet} = the jet zone temperature, K
d_j = the jet zone diameter, m
g = acceleration of gravity, m s^{-2}
u_{or} = the jet velocity at the nozzle, m s^{-1}
d_p = the particle diameter, m
F_{rj}, k, and f_i = the constant defined in Eq. 9
h_j = the jet zone depth, m
V_j = the jet zone volume, m^3
V_d = the annulus dense-phase zone volume, m^3
U_{ex} = the gas exchange rate between the jet zone and the annulus dense-phase zone, m s^{-1}
K = the coefficient defined in Eq. 13
S_a = the cross-sectional area of the annulus dense-phase zone, m^2
u_{mf} = the minimum fluidizing gas velocity, m s^{-1}
u_d = the gas velocity from the distributor shape, m s^{-1}
u_j = the jet gas velocity, m s^{-1}
W_s = the laterally entrained particle flow rate, kg s^{-1}
$W_{s,hj}$ = the solids mass flow rate at the top of the jet zone, kg s^{-1}
W_{g0} = the gas mass flow rate from the nozzle, kg s^{-1}
h = the axial distance from nozzle, m
Q_{ash} = the heat loss caused by sensible heat of ash, J
m^* = the total amount of ash, kg
ΔT = the temperature changing of ash, K
C_{pi} = the heat capacity of each ash component, J kg^{-1} K^{-1}
C_p = the mean heat capacity of ash components, J kg^{-1} K^{-1}
x_i = the mass fraction of each component in ash
k_s = the pre-exponential factor
E = the activation energy, kJ mol^{-1}
T = the reactor temperature, K
t = the residence time, s
c_i = each component in the reactor concentration, mol m^{-3}
A = coal sample
S = the AFB reactor with inner diameter of 300 mm
L = the AFB reactor with inner diameter of 600 mm

Greek letters

λ = the nozzle design coefficient
ρ_s = the particle density, kg m^{-3}
ρ_g = the gas density, kg m^{-3}
ε_{mf} = the voidage of the bed at minimum fluidization
ϕ_r = the cone angle, rad
μ_g = the gas viscosity, Ns m^{-2}
β = the reactor volume scale-up coefficient
β_1 = the total feedstock scale-up coefficient
β_2 = the gas backflow rate scale-up coefficient
β_3 = the jet zone volume scale-up coefficient
β_4 = the annulus dense-phase volume scale-up coefficient

Acronyms

CSTR = the continuous stirred tank reactor
PSR = the perfectly stirred reactor
PFR = the plug flow reactor
Re = Reynolds number

Literature Cited

1. Patel JG. The U-gas® process. *Int J Energy Res.* 1980;4:149–165.
2. Huang JJ, Fang YT, Chen HS, Wang Y. Coal gasification characteristic in a pressurized fluidized bed. *Energy Fuels.* 2003;17:1474–1479.
3. Schwartz CW, Rath LK, Freier MD. Westinghouse gasification process. *Chem Eng Prog.* 1982;78:55–63.
4. Fang YT, Huang JJ, Wang Y, Zhang BJ. Experiment and mathematical modeling of a bench-scale circulating fluidized bed gasifier. *Fuel Process Technol.* 2001;69:29–44.
5. Yang WC, Keairns DL. Operational analysis of ash-agglomerating fluidized bed gasifiers. *Powder Technol.* 2000;111:168–174.
6. Zhao J, Lim CJ, Grace JR. Flow regimes and combustion behaviour in coal-burning spouted and spout-fluid beds. *Chem Eng Sci.* 1987;42:2865–2875.
7. Mısırlıoğlu Z, Canel M, Sınağ A. Hydrogasification of chars under high pressures. *Energy Convers Manage.* 2007;48:52–58.
8. Luo CH, Aoki K, Uemiya S, Kojima T. Numerical modeling of a jetting fluidized bed gasifier and the comparison with the experimental data. *Fuel Process Technol.* 1998;55:193–218.

9. Werther J. Scale-up modeling for fluidized bed reactors. *Chem Eng Sci*. 1992;47:2457–2462.
10. Bisio A, Kabel RL. *Scale-Up of Chemical Processes*. NewYork: Wiley, 1985.
11. Matsen JM. Design and scale-up of CFB catalytic reactors. In: Grace JR, Avidan AA, Knowlton TM, editors. *Circulating Fluidized Beds*. Germany: Springerlink, 1996:489–503.
12. Mabrouk R, Radmanesh R, Chaouki J, Guy C. Scale effects on fluidized bed hydrodynamics. *Int J Chem React Eng*. 2005;3:1–11.
13. Glicksman LR. Fluidized bed scale-up. In: Yang WC, editor. *Fluidization, Solids Handling and Processing: Industrial Applications*. Park Ridge, NJ: Noyes, 1999:1–100.
14. Mithani R, Shenoi S, Fan LT, Walawender WP. Ranking dimensionless groups in fluidized-bed reactor scale-up. *Int J Approx Reason*. 1990;4:69–85.
15. Qi XB, Zhu J, Huang WX. Hydrodynamic similarity in circulating fluidized bed risers. *Chem Eng Sci*. 2008;63:5613–5625.
16. Knowlton TM, Karri SBR, Issangya A. Scale-up of fluidized-bed hydrodynamics. *Powder Technol*. 2005;150:72–77.
17. Stefanova A, Grace JR, Lim CJ, Bi XT, Lim KS, Sanderson J. Scale-up effect on heat transfer. *2007 ECI conference on the 12th International Conference on Fluidization–New Horizons in Fluidization Engineering*. Curran Associates, Inc., Vancouver, Canada, 2007: 273–280.
18. Béttega R, Corrêa RG, Freire JT. Scale-up study of spouted beds using computational fluid dynamics. *Can J Chem Eng*. 2009;87:193–203.
19. Cao JT, Cheng ZH, Fang YT, Jing HM, Huang JJ, Wang Y. Simulation and experimental studies on fluidization properties in a pressurized jetting fluidized bed. *Powder Technol*. 2008;183:127–132.
20. Guenther C, Shahnam M, Syamlal M, Longanbach J, Cicero D, Smith P. CFD modeling of a transport gasifier. *Proceedings of the 19th Annual Pittsburgh Coal Conference*. Curran Associates, Inc., Pittsburgh, Pennsylvania, 2002:24–26.
21. Du W, Xu J, Ji Y, Wei WS, Bao XJ. Scale-up relationships of spouted beds by solid stress analyses. *Powder Technol*. 2009;192:273–278.
22. Wang QC, Zhang K, Brandani S, Jiang JC. Scale-up strategy for the jetting fluidized bed using a CFD model based on two-fluid theory. *Can J Chem Eng*. 2009;87:204–210.
23. Li QJ, Zhang MY, Zhong WQ, Wang XF, Xiao R, Jin BS. Simulation of coal gasification in a pressurized spout-fluid bed gasifier. *Can J Chem Eng*. 2009;87:169–176.
24. Gao K, Wu JH, Wang Y, Zhang DK. Bubble dynamics and its effect on the performance of a jet fluidised bed gasifier simulated using CFD. *Fuel*. 2006;85:1221–1231.
25. Shadle LJ, Berry DA, Syamlal M. *Coal Conversion Processes, Gasification*. NewYork: Wiley, 2002.
26. Wen CY, Chaung TZ. Entrainment coal gasification modeling. *Ind Eng Chem Process Des Dev*. 1979;18:684–695.
27. Li X, Grace JR, Watkinson AP, Lim CJ, Ergüdenler A. Equilibrium modeling of gasification: a free energy minimization approach and its application to a circulating fluidized bed coal gasifier. *Fuel*. 2001; 80:195–207.
28. Liu ZY, Fang YT, Deng SP, Huang JJ, Zhao JT, Cheng ZH. Simulation of pressurized ash agglomerating fluidized bed gasifier using Aspen Plus. *Energy Fuels*. 2012;26:1237–1245.
29. De Lasa HI, Grace JR. The influence of the freeboard region in a fluidized bed catalytic cracking regenerator. *AIChE J*. 1979;25:984–991.
30. Feng J, Hou XC, Chen XH, Jia YL, Li WY. Thermochemical process study on a jet-fluidized-bed gasifier reaction system by an equivalent chemical reactor network. *Energy Fuels*. 2011;25:4063–4069.
31. Reaction Design. *Chemkin Theory Manual: Plug-Flow Assumptions and Equations*. San Diego, CA, 2004:157–162.
32. Kee RJ, Coltrin ME, Glarborg P. *Chemically Reacting Flow: Theory and Practice*. New Jersey: Wiley, 2003.
33. Tsukada M, Horio M. Gas motion and bubble formation at the distributor of a fluidized bed. *Powder Technol*. 1990;63:69–74.
34. Bi JC, Kojima T. Prediction of temperature and composition in a jetting fluidized bed coal gasifier. *Chem Eng Sci*. 1996;51:2745–2750.
35. Yang WC, Keairns DL. Estimating the jet penetration depth of multiple vertical grid jets. *Ind Eng Chem Fundam*. 1979;18:317–320.
36. Mendes A, Dollet A, Ablitzer C, Perrais C, Flamant G. Numerical simulation of reactive transfers in spouted beds at high temperature: application to coal gasification. *J Anal Appl Pyrolysis*. 2008;82:117–128.
37. Merrick D. Mathematical models of the thermal decomposition of coal: 1. The evolution of volatile matter. Fuel. 1983;62:534–539.
38. Suuberg EM, Peters WA, Howard JB. Product compositions in rapid hydropyrolysis of coal. *Fuel*. 1980;59:405–412.
39. Yu L, Lu J, Zhang XP, Zhang SJ. Numerical simulation of the bubbling fluidized bed coal gasification by the kinetic theory of granular flow (KTGF). *Fuel*. 2007;86:722–734.
40. Gerun L, Paraschiv M, Vîjeu R, Bellettre J, Tazerout M, Gøbel B, Henriksen U. Numerical investigation of the partial oxidation in a two-stage downdraft gasifier. *Fuel*. 2008;87:1383–1393.
41. Chejne F, Hernandez JP. Modelling and simulation of coal gasification process in fluidised bed. *Fuel*. 2002;81:1687–1702.
42. Kimura T, Kojima T. Numerical model for reactions in a jetting fluidized bed coal gasifier. *Chem Eng Sci*. 1992;47:2529–2534.
43. Watkinson A, Lucas J, Lim C. A prediction of performance of commercial coal gasifiers. *Fuel*. 1991;70:519–527.
44. Macak J, Malecha J. Mathematical model for the gasification of coal under pressure. *Ind Eng Chem Process Des Dev*. 1978;17:92–98.
45. Bayarsaikhan B, Hayashi J, Shimada T, Sathe C, Li C, Tsutsumi A, Chiba T. Kinetics of steam gasification of nascent char from rapid pyrolysis of a Victorian brown coal. *Fuel*. 2005;84:1612–1621.
46. Mühlen H-J, van Heek KH, Jüntgen H. Kinetic studies of steam gasification of char in the presence of H2, CO2 and CO. *Fuel*. 1985;64: 944–949.
47. Mann MD, Knutson RZ, Erjavec J, Jacobsen JP. Modeling reaction kinetics of steam gasification for a transport gasifier. *Fuel*. 2004;83: 1643–1650.
48. Deng Z, Xiao R, Jin B, Huang H, Shen L, Song Q, Li Q. Computational fluid dynamics modeling of coal gasification in a pressurized spout-fluid bed. *Energy Fuels*. 2008;22:1560–1569.
49. Fang YT, Feng J. The fundamental research of large-scale coal gasification technology applied to the polygeneration system. China: 973 Project Report (2005CB22120102), 2010.
50. He YL, Lim CJ, Grace JR. Scale-up studies of spouted beds. *Chem Eng Sci*. 1997;52:329–339.
51. Glicksman LR, Hyre MR, Farrell PA. Dynamic similarity in fluidization. *Int J Multiphase Flow*. 1994;20:331–386.
52. Horio M, Nonaka A, Sawa Y, Muchi I. A new similarity rule for fluidized bed scale-up. *AIChE J*. 1986;32:1466–1482.

Manuscript received July 16, 2013, and revision received Jan. 9, 2014.